NRC·CNRC

NRC Publications Archive
Archives des publications du CNRC

Field measurements of boundary-layer flows in ventilated rooms

Zhang, J. S.; Shaw, C. Y.; Nguyen-Thi, L. C.; MacDonald, R. A.; Kerr, G.

This publication could be one of several versions: author's original, accepted manuscript or the publisher's version. / La version de cette publication peut être l'une des suivantes : la version prépublication de l'auteur, la version acceptée du manuscrit ou la version de l'éditeur.

Publisher's version / Version de l'éditeur:

ASHRAE Transactions, 101, Pt. 2, pp. 1-9, 1995

NRC Publications Record / Notice d'Archives des publications de CNRC:
https://nrc-publications.canada.ca/eng/view/object/?id=1662854d-ef53-4221-be90-e1943fc5148d
https://publications-cnrc.canada.ca/fra/voir/objet/?id=1662854d-ef53-4221-be90-e1943fc5148d

Access and use of this website and the material on it are subject to the Terms and Conditions set forth at
https://nrc-publications.canada.ca/eng/copyright
READ THESE TERMS AND CONDITIONS CAREFULLY BEFORE USING THIS WEBSITE.

L'accès à ce site Web et l'utilisation de son contenu sont assujettis aux conditions présentées dans le site
https://publications-cnrc.canada.ca/fra/droits
LISEZ CES CONDITIONS ATTENTIVEMENT AVANT D'UTILISER CE SITE WEB.

Questions? Contact the NRC Publications Archive team at PublicationsArchive-ArchivesPublications@nrc-cnrc.gc.ca. If you wish to email the authors directly, please see the first page of the publication for their contact information.

Vous avez des questions? Nous pouvons vous aider. Pour communiquer directement avec un auteur, consultez la première page de la revue dans laquelle son article a été publié afin de trouver ses coordonnées. Si vous n'arrivez pas à les repérer, communiquez avec nous à PublicationsArchive-ArchivesPublications@nrc-cnrc.gc.ca.

National Research Council Canada | Conseil national de recherches Canada

Canada

NRC·CNRC Institute for Research in Construction
CNRC·NRC Institut de recherche en construction
http://www.nrc-cnrc.gc.ca/irc

Field measurements of boundary-layer flows in ventilated rooms

NRCC-37883

Zhang, J.S.; Shaw, C.Y.; Nguyen-Thi, L.C.; MacDonald, R.A.; Kerr, G.

July 1995

A version of this document is published in / Une version de ce document se trouve dans:
ASHRAE Transactions, 101, (Pt. 2), pp. 1-9, 1995

The material in this document is covered by the provisions of the Copyright Act, by Canadian laws, policies, regulations and international agreements. Such provisions serve to identify the information source and, in specific instances, to prohibit reproduction of materials without written permission. For more information visit http://laws.justice.gc.ca/en/showtdm/cs/C-42

Les renseignements dans ce document sont protégés par la Loi sur le droit d'auteur, par les lois, les politiques et les règlements du Canada et des accords internationaux. Ces dispositions permettent d'identifier la source de l'information et, dans certains cas, d'interdire la copie de documents sans permission écrite. Pour obtenir de plus amples renseignements : http://lois.justice.gc.ca/fr/showtdm/cs/C-42

National Research Council Canada | Conseil national de recherches Canada
Canada

FIELD MEASUREMENTS OF BOUNDARY-LAYER FLOWS IN VENTILATED ROOMS

Jianshun S. Zhang, Ph.D.
Associate Member ASHRAE

C.Y. Shaw, Ph.D., P.E.
Member ASHRAE

Lan C. Nguyen-Thi, P.E.
Associate Member ASHRAE

Robert A. MacDonald

Gemma Kerr, Ph.D.
Member ASHRAE

ABSTRACT

Profiles of air velocity and turbulent kinetic energy near the surfaces of walls, ceilings, floors, and furnishings were measured under field conditions for four space layouts of an office building: a partitioned office room, a single office room, a small conference room, and a computer room. Three types of flows near the surfaces were identified based on the measured data: (1) near-stagnant flow that had mean velocities and turbulent kinetic energies of less than 0.05 ±0.025 m/s (10 ± 5 fpm) and 0.001 ± 0.001 (m/s)^2 (38.75 ±38.75 (fpm)^2], respectively; (2) weak turbulence flow that had mean velocities and turbulent kinetic energies from 0.05 ± 0.025 to 0.25 ± 0.05 m/s (10 ± 5 to 50 ± 10 fpm) and from 0.001 ± 0.001 to 0.01 ± 0.002 (m/s)^2 (38.75 ± 38.75 to 387.5 ± 77.5 [fpm]^2), respectively; and (3) strong turbulence flow that had velocities and turbulent kinetic energies higher than 0.25 ± 0.05 m/s (50 ± 10 fpm) and 0.01 ±0.002 (m/s)^2 (387.5 ± 77.5 [fpm]^2), respectively. The results are useful for establishing realistic airflow conditions in testing and modeling contaminant emission from building materials and indoor furnishings.

INTRODUCTION

Many boundary layer flows exist in ventilated rooms, such as airflows near the surfaces of walls, floors, ceilings, desks, partitions, etc. The flow characteristics of these boundary layers play an important role in determining the rates of mass and heat transfer between these surfaces and the ambient air. For example, the boundary-layer flows would affect the emission rate of volatile organic compounds (VOCs) from building materials and indoor furnishings (Zhang et al. 1993). Knowledge of the boundary-layer flow characteristics under field conditions is essential for establishing realistic airflow conditions for testing and modeling the rates of VOC emissions from the surfaces of building materials and indoor furnishings (ASTM 1990).

The airflow characteristics in ventilated rooms have been measured under both laboratory and field conditions (e.g., Matthews et al. 1987; Melikov et al. 1988; Sandberg 1989; Whittle and Clancy 1991; Zhang et al. 1992). These measurements were primarily aimed at examining the conditions in the occupied region or the air distributions within the entire room. Recently, Sandberg et al. (1991) measured the mean velocity and turbulence distribution near the ceiling surface where a wall jet was present using a full-scale empty test room (3.6 m by 4.2 m by 2.5 m [11.8 ft by 13.8 ft by 8.2 ft]). However, field data of the airflow characteristics near the surfaces of walls, floors, ceilings, and internal furnishings are lacking.

In this study, the profiles of velocity and turbulent kinetic energy were measured under field conditions for the boundary-layer flows near the surfaces of walls, floors, ceilings, and furnishings in four space layouts of an office building: a partitioned office room, a single office room, a small conference room, and a computer room. The objectives were to determine the range of velocity and turbulence levels and their characteristics near the surfaces under realistic ventilation conditions and provide field data for developing empirical models of the boundary-layer flows. The results will be useful for establishing proper airflow conditions in conducting material emission tests using small or large chambers and developing methods to extrapolate the chamber test data to predict the VOC emission rates in real environments.

METHODS AND PROCEDURES

Test Rooms and Measurement Conditions

Measurements were conducted for the following typical room layouts:

Room A: a partitioned office room with two ceiling linear diffusers and two ceiling return slots (Figure 1),

Room B: a single office room with a floor-mounted air supply diffuser and a high wall-mounted return grille (Figure 2),

Room C: a small conference room with four ceiling linear diffusers and four ceiling return slots (Figure 3), and

Room D: a computer room with a ceiling-mounted square radial diffuser and a high wall-mounted return slot (Figure 4).

Jianshun S. Zhang is a research associate, **C.Y. Shaw** is a senior researcher, and **Robert A. MacDonald** is a senior technical officer at the National Research Council, Canada, Ottawa, ON, . **Lan Chi Nguyen-Thi** is an internal environment engineer-in-training and **Gemma Kerr** is an environmental chemist at Public Works and Government Services Canada, Ottawa, ON.

THIS PREPRINT IS FOR DISCUSSION PURPOSES ONLY, FOR INCLUSION IN ASHRAE TRANSACTIONS 1995, V. 101, Pt. 2. Not to be reprinted in whole or in part without written permission of the American Society of Heating, Refrigerating and Air-Conditioning Engineers, Inc., 1791 Tullie Circle, NE, Atlanta, GA 30329. Opinions, findings, conclusions, or recommendations expressed in this paper are those of the author(s) and do not necessarily relect the views of ASHRAE. Written questions and comments regarding this paper should be received at ASHRAE no later than **July 5, 1995.**

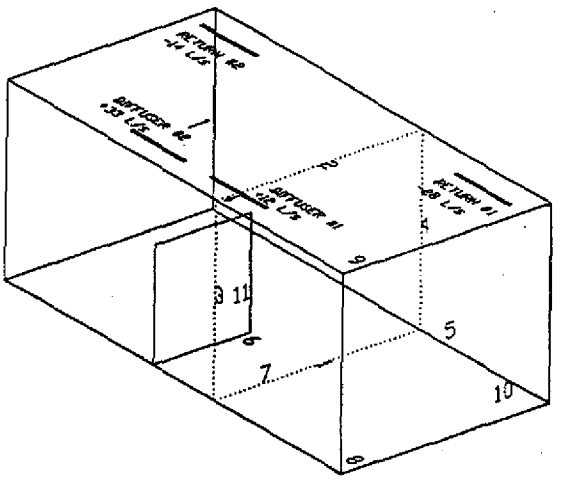

Figure 1 *Schematic and picture of room A: 7.6 m by 3.7 m by 3.0 m (25 ft by 12 ft by 10 ft). The partition dimensions are 1626 mm by 64 mm by 1829 mm (64 in. by 2.5 in. by 72 in.) and measurement locations are indicated by the numbers.*

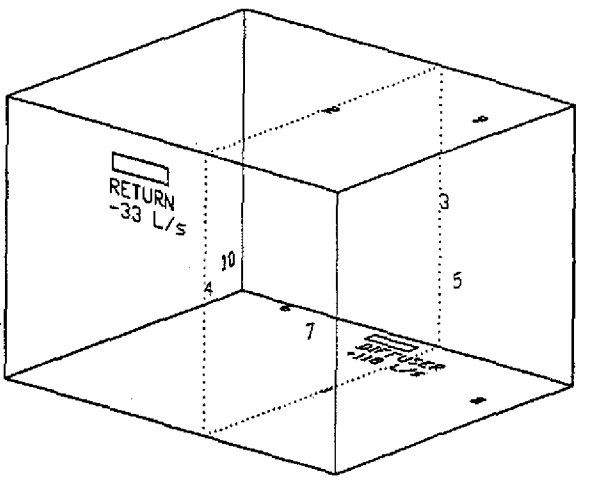

Figure 2 *Schematic and picture of room B: 4.6 m by 3.7 m by 3.0 m (15 ft by 12 ft by 10 ft). Measurement locations are indicated by the numbers.*

All four rooms were located in the same building. The ventilation system of the building operated under normal conditions on workdays (i.e., no special adjustment to the HVAC system). The furnishings in the rooms were unaltered and doors were closed during the measurements. The rooms were unoccupied during the velocity measurements. Airflow rates through each diffuser and return were measured using a flow hood and are shown in Figures 1 through 4. Room air temperature and humidity were also measured using a psychrometer for all measurement locations (Table 1). All the surfaces investigated were not apparent heat sources (e.g., light fixtures, walls heated by solar radiation or radiant heating panels, etc.) or sinks (e.g., cold surfaces of exterior walls in winter, cooling panels, etc.). Temperatures over the measurement surfaces were estimated to be within 1°C (1.8°F) of the ambient air temperature as under normal room conditions.

Measurement Locations

In order to cover a wide range of velocity and turbulence conditions near surfaces of walls, ceilings, floors, and internal furnishings, measurements were made for the following locations in each room:

1. centrally located and near the floor surface in the "main airflow path,"
2. centrally located and near the ceiling surface in the "main airflow path,"
3. centrally located and near a wall surface in the "main airflow path,"
4. centrally located and near the wall surface opposite that of no. 4 in the "main airflow path,"
5. centrally located and near a wall surface that is not in the "main airflow path,"
6. near a desktop surface,
7. under a desk near a side (vertical) surface (rooms A, B, and D) or near a bottom (horizontal) surface (room C),

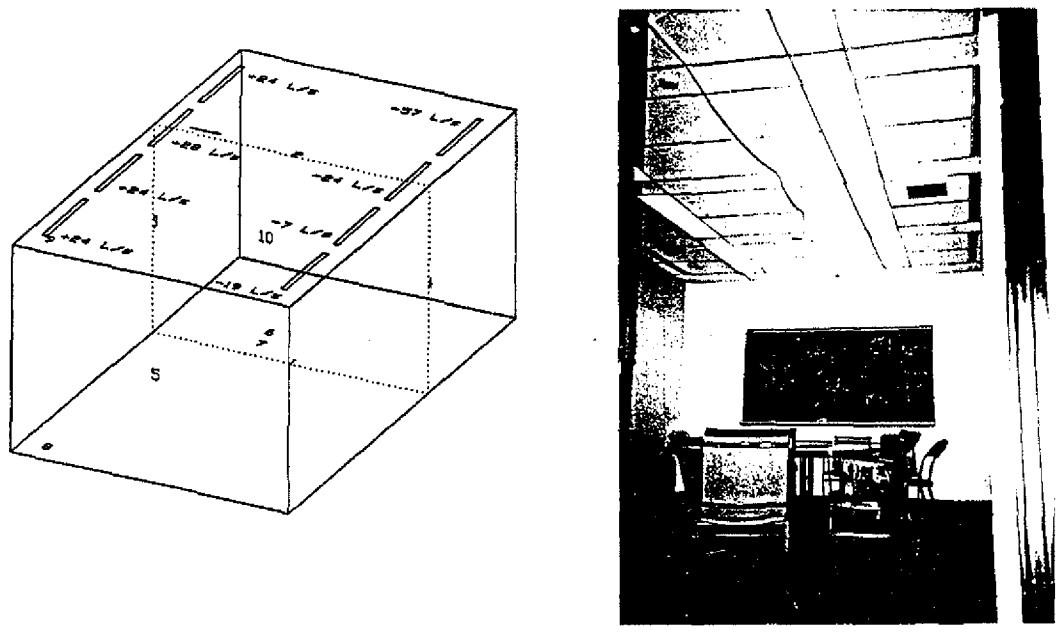

Figure 3 *Schematic and picture of room C: 6.7 m by 4.1 m by 3.0 m (22 ft by 13.5 ft by 10 ft). Measurement locations are indicated by the numbers.*

8. near a floor surface at a corner,
9. near a ceiling surface at a corner,
10. near a wall surface at a corner, and
11. near a surface of room partitions (for room A only).

It should be noted that the "main airflow path" mentioned (also indicated in Figures 1 through 4 by dotted lines) was an anticipated one that was based solely on the locations of supply air diffuser(s) and return air grille(s). It was not necessarily the actual main airflow path in the room because the actual room airflow pattern was also affected by the air leakages (mainly those through doors) and internal furnishings. We used the "main airflow path" mentioned mainly for the convenience of identifying those measurement locations that were most likely experiencing relatively high air velocities near the surfaces.

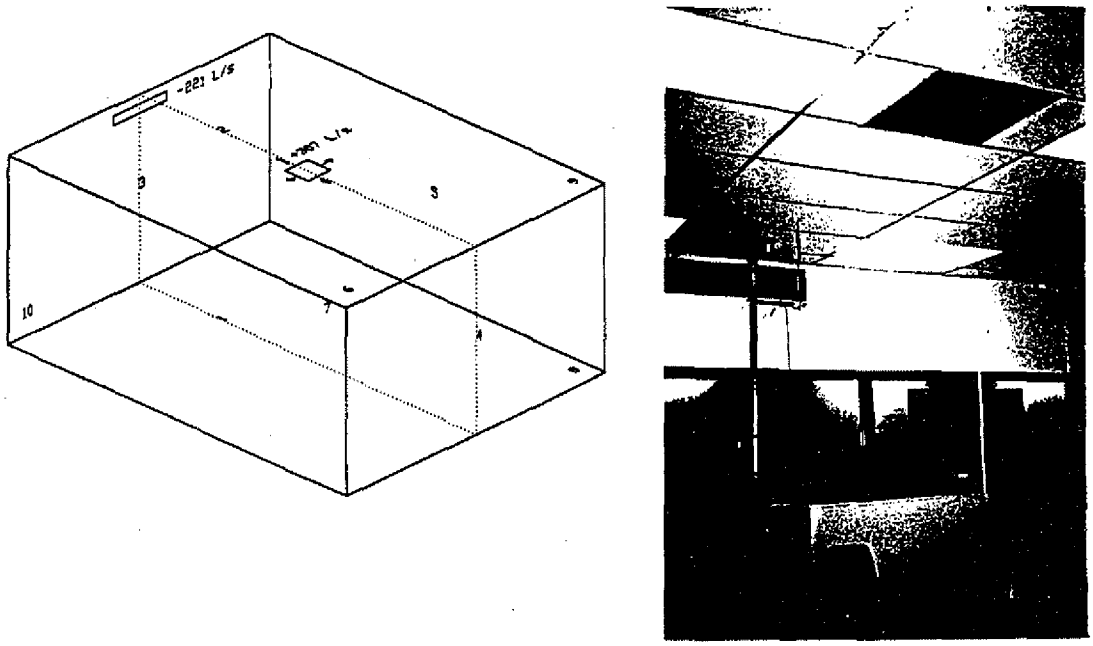

Figure 4 *Schematic and picture of room D: 6.7 m by 5.3 m by 3.0 m (22 ft by 17.5 ft by 10 ft). Measurement locations are indicated by the numbers.*

TABLE 1
Local Air Temperature and Humidity Conditions at Measured Locations

Location	Room A		Room B		Room C		Room D	
No.	T, °C	RH, %	T, °C	RH, %	T, °C	RH, %	T, °C	RH, %
1	23.8	33	22.0	35	21.6	41	19.8	52
2	23.5	36	23.1	40	22.3	39	19.5	50
3	24.3	34	23.1	28	22.0	34	18.5	53
4	24.2	34	22.6	32	21.7	39	19.1	47
5	24.3	38	23.0	34	22.0	40	19.0	41
6	24.3	38	22.9	30	22.2	37	19.0	40
7	24.3	38	22.9	28	21.6	38	19.7	46
8	23.4	34	22.1	37	21.6	39	20.0	51
9	24.2	37	22.6	30	22.0	40	20.0	51
10	24.3	38	23.0	29	21.7	39	19.8	50
11	24.3	38						
Avg	24.1	36	22.7	32	21.9	39	19.4	48
Std	0.3	2	0.4	4	0.2	2	0.5	4

For each of the mentioned locations, measurements were made 2.5, 5.0, 7.5, 10.0, 12.5, 15.0, 17.5, 20.0, 22.5, 25.0, 27.5, 30.0, 35.0, 40.0, 45.0, 50.0, 60.0, 70.0, 80.0, 90.0, and 100.0 mm from the surface—a total of 21 points per location. The probe was moved perpendicularly away from the surface from one point to another using a traversing system driven by a stepping motor. The stepping motor was either controlled by a personal computer (for vertical traversing) or a manual switching box (for horizontal traversing). Data acquisition and probe traversing were performed using the menu-driven C program "ROOMAIR," developed in-house.

Measurement Method

A single-component hot-wire probe (a straight type with a wire diameter of 5 μm) was used to measure the instantaneous air velocity with a sampling rate of 20 Hz and a sampling period of 204.8 seconds, which resulted in 4,096 data for each measured point. Neutrally buoyant smoke generated by titanium tetrachloride was used to determine the local primary airflow direction 20.0 mm (0.79 in.) from the surface over which the profiles of air velocity and turbulent kinetic energy were to be measured. The hot-wire probe was then aligned with the flow so that the wire was perpendicular to the local primary airflow direction for velocity measurements. This minimized the effect of the probe's angle sensitivity on the measurement accuracy.

It was observed that the local primary airflow direction 20.0 mm (0.79 in.) from the surface was relatively stable when the local air velocity was greater than about 0.1 m/s (20 fpm) but less stable for a lower local air velocity. However, a previous study (Zhang et al. 1991) showed that the angle sensitivity of the wire probe is minimal when the velocity is lower than 0.1 m/s (20 fpm). Additionally, the probe's operating temperature was set at 120°C (248°F) instead of 250°C (482°F), as commonly used in hot-wire anemometry. This would reduce the effect of natural convection (due to the heated wire itself) on the measurement accuracy. Zhang et al. (1991) found that the detection limit for a hot-wire probe operating at 200°C (392°F) was about 0.05 m/s (10 fpm) due to the natural convection effect (i.e., the heated wire probe induces a convective flow that "contaminates" the airflow to be measured). For the present study, the detection limit was found to be about 0.025 m/s (5 fpm) since a much lower probe operating temperature (120°C vs. 200°C [248°F vs. 392°F]) was used. The probe was calibrated before the measurements for the range of 0.025 to 1.25 m/s (5 to 246 fpm) using a small wind tunnel designed for low-velocity calibrations (TSI 1989). The overall accuracy of the velocity measurements for this study was estimated to be within ±25% or ±0.015 m/s of the measured value, whichever is higher in absolute error. This means that at the low end of the velocity range (0.025 m/s [5 fpm]), the measurement error could be as high as ±60%. This error estimation was based on the capability of the hot-wire anemometry (Zhang et al. 1991) and the airflow features studied. Room airflows under field conditions are usually not as stable as those under well-controlled laboratory conditions.

Data Analysis

The instantaneous air velocities measured were used to calculate the following parameters.

Mean air velocity:

$$U = \frac{1}{n}\sum_{i=1}^{n} u_i \qquad (1)$$

where

U = mean air velocity (m/s),
u_i = instantaneous air velocity (m/s), and
n = total number of data (4,096 in this study).

Turbulent kinetic energy:

$$U = \frac{1}{n}\sum_{i=1}^{n}(u_i - U)^2 \qquad (2)$$

where

k = turbulent kinetic energy, $(m/s)^2$.

The turbulent kinetic energy as defined here is a measure of the turbulence level in the flow. The data analysis was performed using a C program named "ROOMVENT," which was developed in house. ROOMVENT can directly process the data collected by the program "ROOMAIR."

RESULTS AND DISCUSSION

Room A

As shown in Figure 5, location 3 had the highest levels of air velocity near the surface (e.g., about 0.3 m/s at y = 20.0 mm). This was due to the airflow from diffuser 1 (Figure 1). The shape of the mean velocity profile for location 3 indicates a power law relationship between velocity and distance from the surface (i.e., $U = ay^b$, where a and b are constants). The highest velocity gradient occurred between y = 0 mm and 12.5 mm. This may be regarded as the inner region in which the viscous effect is dominant, as in fully developed boundary layer flows over a flat plate (see Kays and Crawford 1980). Farther away from the surface, the velocity gradient decreased as y increased, and the gradient approached zero (i.e., velocity approached maximum) at about y = 80.0 mm. The region from y = 12.5 mm to 80.0 mm may be regarded as the outer region of the boundary layer where the turbulent effect dominates the viscous effect. The total boundary layer thickness for location 3 was about 80.0 mm.

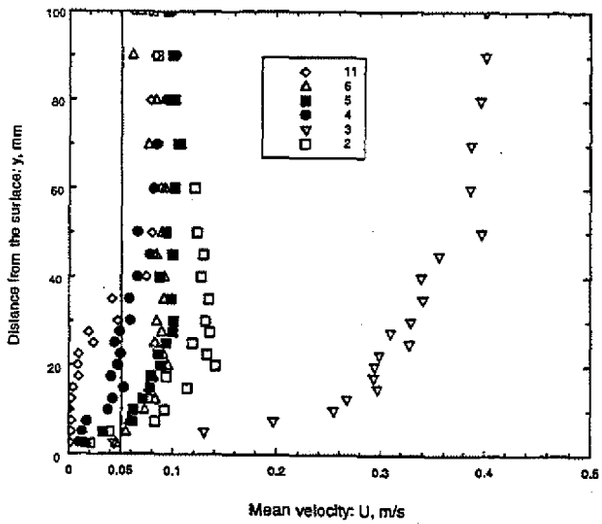

Figure 5 *Measured mean velocities for room A (U < 0.05 m/s for locations 1, 7, 8, 9, and 10, and is not shown for clarity).*

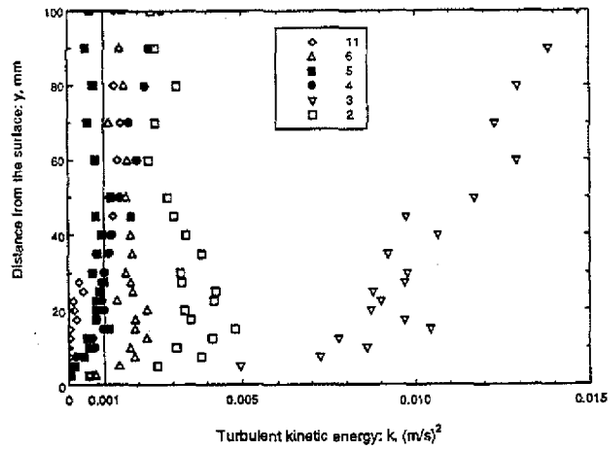

Figure 6 *Measured turbulent kinetic energy for room A (k < 0.001 $[m/s]^2$ for locations 1, 7, 8, 9, and 10, and is not shown for clarity).*

The profile of turbulent kinetic energy (Figure 6) for location 3 shows a local peak at y = 15.0 mm. The local peak appears to be due to the turbulence production near the surface instead of measurement uncertainties since the peak location (i.e., y = 15.0 mm) corresponds to the transition region between the inner and outer regions of the boundary layer as discussed above. Farther away from the surface (y > 20.0 mm, i.e., after the local peak), the turbulent kinetic energy became more scattered and increased with y to about 0.015 $(m/s)^2$. This indicates that there was stronger turbulence in the ambient airstream than in the boundary-layer flow near the surface. Based on the theory of turbulence transport (Hinze 1975), the turbulence in the ambient airstream was a combination of the turbulence produced locally by the velocity gradient near the surface and that transported from upstream of the flow. In the case of location 3, it may be expected that there was strong turbulence production upstream because of the impingement of the diffuser air jet on the wall surface.

Figure 5 also shows that locations 2, 4, 5, and 6 had medium levels of air velocity near the surface (0.05 to 0.12 m/s). Each profile shows that local maximum velocities were reached at approximately y = 20.0 ± 5.0 mm for these locations, which was much less than y = 80.0 mm in location 3. The turbulent kinetic energies at locations 2, 4, 5, and 6 were between 0.001 and 0.005 $(m/s)^2$, as shown in Figure 6. Although quite scattered, the data show that the turbulent kinetic energy was higher near the surfaces (e.g., at y = 10.0 to 20.0 mm) than in the ambient airstreams (e.g., y > 40.0 mm) for locations 2 and 6, but this was not true for locations 4 and 5, which had turbulent kinetic energy rates of only about 0.001 $(m/s)^2$ at y = 20.0 mm. This means that the local turbulent kinetic energy near the surfaces can be different even though the local air velocity is in a similar level, depending on the turbulence level in the ambient airstreams.

It is interesting to note that, at location 11, the mean velocity remained essentially zero from the surface out to about 20.0 mm and then increased with the distance farther away from the surface. This was likely due to the effect of the rough surface of the partition. The partition's surface was made of a coarsely woven fiber material that appeared to present more resistance to the airflow than the other solid surfaces.

The remaining locations (1, 7, 8, 9, and 10) had the lowest air velocity levels (< 0.05 m/s) and turbulent kinetic energy (< 0.001 $[m/s]^2$) near the surfaces (data for these locations are not shown in the figures for clarity). The gradient-type velocity profile cannot be clearly identified for these locations; hence, the flows over the surfaces may be regarded as essentially stagnant. We will call them "near-stagnant flows" because of their small but measurable velocity and turbulence. These low-velocity locations included the location under the desk (7) and the three locations at room corners (8, 9, and 10). Location 1, which was in the "main airflow path" (not necessarily the real one, as discussed before), also had the lowest velocity and turbulence level. This was probably due to the fact that diffuser 1 only had a supply airflow rate of 12 L/s and that the airflows from diffuser 2 could not reach location 1.

Room B

As shown in Figures 7 and 8, locations 1, 2, 5, 8, and 9 had air velocities in the range of 0.05 to 0.2 m/s and turbulent kinetic energy in the range of 0.001 to 0.004 $(m/s)^2$. Local peaks near the surfaces cannot be clearly seen from the profiles of turbulent kinetic energy for these locations. The thicknesses of the boundary layers for these locations ranged from about 10.0 to 20.0 mm. The remaining locations had velocities of less than 0.05 m/s and turbulent kinetic energy levels of less than 0.001 $(m/s)^2$, which are classified as the "near-stagnant flow" regime discussed above.

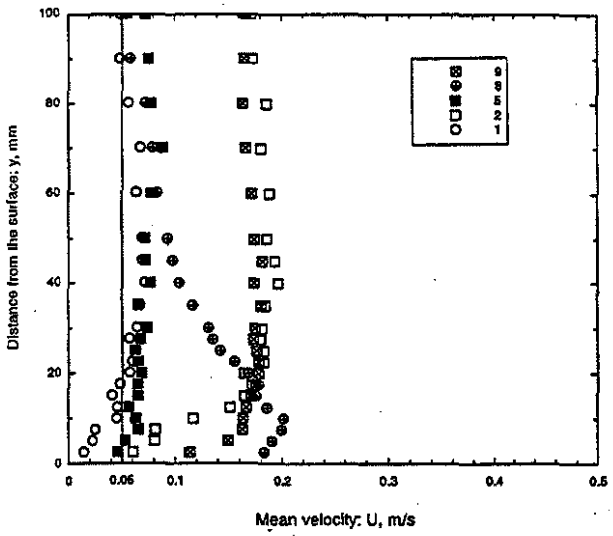

Figure 7 *Measured mean velocities for room B (U < 0.05 m/s for locations 3, 4, 6, 7, and 10, and is not shown for clarity).*

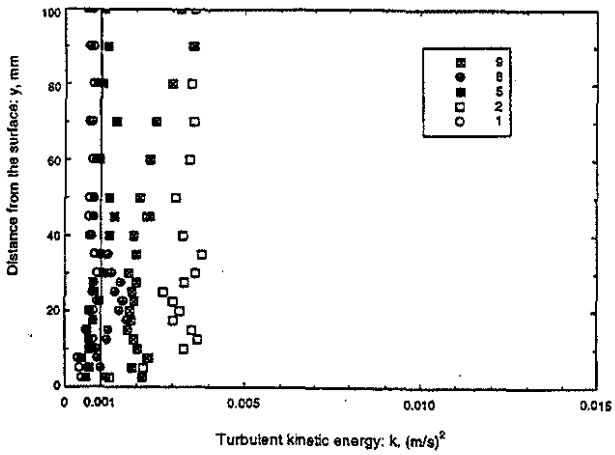

Figure 8 *Measured turbulent kinetic energy for room B (k < 0.001 $[m/s]^2$ for locations 3, 4, 6, 7, and 10, and is not shown for clarity).*

Note that location 8 had a velocity profile that reached its maximum value at 10.0 mm from the surface and then dropped quickly as the distance from the surface increased further, behaving like a strong wall-jet-type flow. However, the corresponding turbulent kinetic energy (Figure 8) was quite low (about 0.001 $[m/s]^2$) at y = 10.0 mm and did not show a local peak near the surface. It was not clear what had caused such a complex flow feature. It might be due to the instability of the mean flow.

It should be noted that locations 1, 2, 3, and 4 were not in the actual main airflow path created by the air diffuser because the desk and file cabinet were in the way (Figure 2). Therefore, relatively high velocity conditions such as in location 3 of room A were not observed in room B, although the airflow rate supplied by the diffuser was relatively high (118 L/s).

Room C

As shown in Figures 9 and 10, locations 1, 2, 3, 4, 6, and 8 had air velocity levels in the range of 0.05 to 0.12 m/s and relatively low levels of turbulent kinetic energy (0.001 to 0.002 $[m/s]^2$). The profiles of turbulent kinetic energy did not show a local peak near the surfaces either. The thickness of the boundary layers for these locations ranged from 10.0 to 30.0 mm. The remaining locations had velocities of less than 0.05 m/s and turbulent kinetic energy of less than 0.001 $(m/s)^2$.

Room D

As shown in Figure 11 (note the different scale used in the graph as compared to that in Figure 5), location 2 had the highest air velocity level near the surface (about 0.95 m/

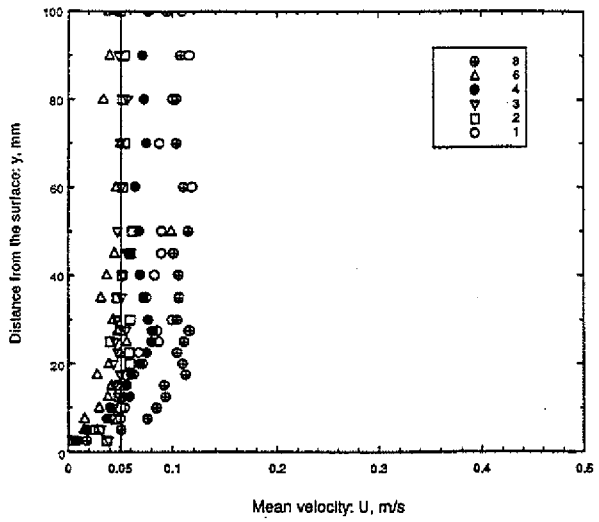

Figure 9 *Measured mean velocities for room C (U < 0.05 m/s for locations 5, 7, 9, and 10, and is not shown for clarity).*

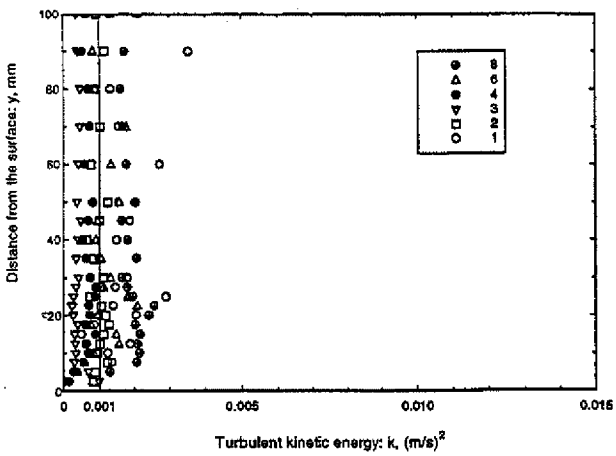

Figure 10 *Measured turbulent kinetic energy for room C (k < 0.001 [m/s]² for locations 5, 7, 9, and 10, and is not shown for clarity).*

s at y = 20.0 mm). The mean velocity profile is similar to that of location 3 in room A, but with thinner inner (y =0 to 5.0 ± 2.5 mm) and outer (y = 5 ± 2.5 to 50.0 mm) layers due to the higher magnitude of air velocity near the surface. The maximum turbulent kinetic energy (Figure 12) near the surface for location 2 was about 0.06 $(m/s)^2$. It occurred at y = 2.5 mm, indicating that the local peak would be somewhere at y _ 2.5 mm. The turbulent kinetic energy decreased as the distance (y) from the surface increased until it reached a magnitude similar to that in the ambient airstream at approximately y = 50.0 mm. This means that the turbulence produced by the surface effect was stronger than that in the ambient airstream. This was apparently due to the large velocity gradient very close to the surface, according to the turbulence theory (Hinze 1975). The high velocity near the

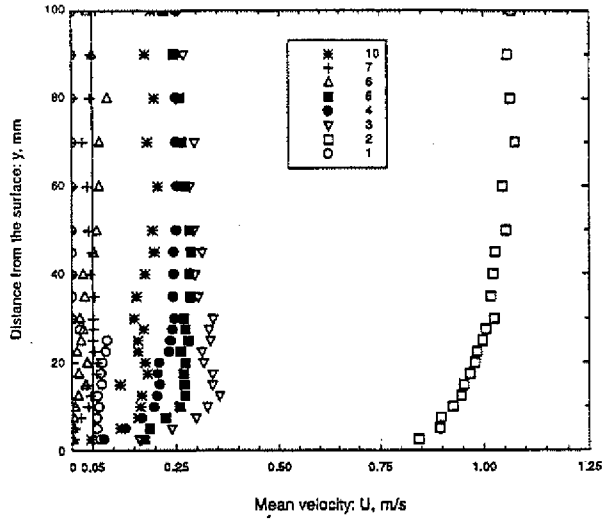

Figure 11 *Measured mean velocities for room D (U < 0.05 m/s for locations 8 and 9 and is not shown for clarity).*

surface was due to the strong jet created by the square radial diffuser at the ceiling.

Location 3 also had a relatively high turbulent kinetic energy near the surface (maximum of 0.016 $[m/s]^2$ at y = 7.5 mm), but its mean velocity profile resembled a wall-jet-type flow with a maximum velocity of 0.35 m/s at about y = 10.0 mm. Its profile of turbulent kinetic energy also showed a clear peak near the surface, indicating a strong turbulence production there.

Locations 4, 5, and 10 had air velocities near the surfaces in the range of 0.15 to 0.35 m/s. The thickness of the boundary layers varied from approximately 10.0 to 30.0 mm. These locations had relatively low turbulent kinetic energy (0.002 to 0.006 $[m/s]^2$). A local peak near the surface can also be seen in the profile of turbulent kinetic

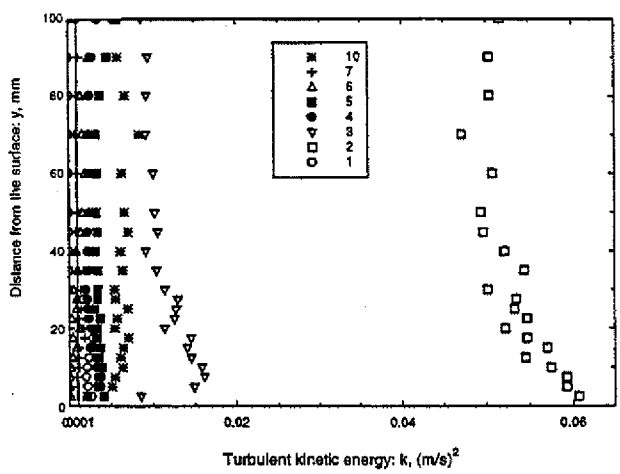

Figure 12 *Measured turbulent kinetic energy for room D (k < 0.001 [m/s]² for locations 8 and 9 and is not shown for clarity).*

energy for location 4 due to the relatively low level of turbulence in the ambient airstream as compared to locations 5 and 10, which had similar levels of mean velocity.

Locations 6 and 7 had velocities of about 0.05 m/s and turbulent kinetic energy of about 0.001 $(m/s)^2$ near the surfaces. The remaining locations had velocity levels of less than 0.05 m/s and turbulent kinetic energy of less than 0.001 $(m/s)^2$ near the surfaces. The data for location 1 were peculiar for some unidentified reasons and were therefore excluded in the analyses.

SUMMARY AND CONCLUSIONS

The measured flow conditions near the surfaces may be summarized into the following three types.

Near-Stagnant Flow This type of flow had velocities near the surface of less than 0.05 ± 0.025 m/s (10 ± 5 fpm). The measured mean velocity profiles near the surface did not show the apparent gradient type of profile similar to that in boundary-layer flows. The turbulent kinetic energy near the surfaces was less than 0.001 ± 0.001 $(m/s)^2$ (38.75 ±38.75 $[fpm]^2$). This type of flow typically occurs near surfaces at corners and under desks.

Weak Turbulence Flow This type of flow had a medium range of velocities (0.05 ± 0.025 to 0.25 ± 0.05 m/s [10 ± 5 to 50 ± 10 fpm]) near the surfaces. The turbulent kinetic energy near the surfaces varied from less than 0.001± 0.001 to 0.01 ± 0.002 $(m/s)^2$ (38.75 ± 38.75 to 387.5 ±77.5 $[fpm]^2$), depending on the turbulence level in the ambient airstreams. These turbulence levels were also moderate compared to those in the ambient airstreams. The thickness of the entire boundary layer was less than 25.0 ±5.0 mm (0.98 ± 0.20 in.). This type of flow typically occurs near surfaces in the open spaces outside the primary airflow field created by the diffuser air jets.

Strong Turbulence Flow This type of flow had relatively high air velocities (greater than 0.25 ± 0.05 m/s [50 ± 10 fpm]) and turbulent kinetic energy (greater than 0.01 ±0.002 $[m/s]^2$ [387.5 ± 77.5 $(fpm)^2$]). The mean velocity profiles either clearly showed inner and outer layers, as in the fully developed turbulent boundary layer flow over a flat plate (location 3 of room A and location 2 of room D), or a wall-jet-type flow with a maximum velocity close to the wall (location 3 of room D). An important common feature of this type of flow appeared to be that a local peak of turbulent kinetic energy could be clearly identified near the surface, indicating a strong turbulence production due to the surface effect. The relatively high velocities near the surfaces were created by the diffuser air jets. This type of flow typically occurs near surfaces that are within the primary airflow field created by diffuser air jet(s).

It should be noted that the four rooms included in this study were selected to generically represent a majority of office space configurations. The 11 locations measured in each room were also chosen to represent a broad range of boundary-layer flow conditions except those over heated or cooled surfaces (i.e., apparent nonisothermal surface conditions). The results presented in this paper can be used to represent the characteristics of boundary-layer flows in real rooms under similar conditions. They are useful for establishing realistic airflow conditions for testing and modeling the contaminant emissions from the surfaces of building materials and indoor furnishings.

ACKNOWLEDGMENTS

This study was sponsored by Public Works/Government Services Canada (PW/GSC) and the National Research Council Canada.

REFERENCES

ASTM. 1990. *Standard guide for small-scale environmental chamber determinations of organic emissions from indoor materials and products*. Philadelphia: American Society for Testing and Materials.

Hinze, J.O. 1975. *Turbulence*, 2d ed. New York: McGraw-Hill.

Kays, W.M., and M.E. Crawford. 1980. *Convective heat and mass transfer*. New York: McGraw-Hill.

Matthews, T.J., C.V. Thompson, D.L. Wilson, A.R. Hawthorne, and D.T Mage. 1987. Air velocities inside domestic environments: An important parameter for passive monitoring. *Indoor Air '87—Proceedings of the 4th International Conference on Indoor Air Quality and Climate*, vol. 1, pp. 154-158. Berlin: Institute for Water, Soil and Air Hygiene.

Melikov, A.K., H. Hanzawa, and P.O. Fanger. 1988. Airflow characteristics in the occupied zone of heated spaces without mechanical ventilation. *ASHRAE Transactions* 94(1): 52-70.

Sandberg, M. 1989. Velocity characteristics in mechanically ventilated office rooms. In *Room Vent '87, Proceedings of 1st International Conference of Air Distribution in Ventilated Spaces*, Stockholm, Sweden.

Sandberg, M., C. Blomquist, and M. Mattson. 1991. Turbulence characteristics in rooms ventilated with a high velocity jet. *Air Movement and Ventilation Control Within Buildings, Proceedings of 12th AIVC Conference*, vol. 2, pp. 105-124.

TSI. 1989. *Model 8390 benchtop wind tunnel: Operation and service manual*. St. Paul, MN: TSI Inc.

Whittle, G.E., and E.M. Clancy. 1991. Evaluation of cases B, D, E—Presentation of results from measurements and simulations. IEA Annex 20 Research Report No. 1.22.

Zhang, J.S., L.L. Christianson, and G.J. Wu. 1991. Hot wire/film anemometry for room air motion studies. *Air Movement and Ventilation Control Within Buildings, Proceedings of 12th AIVC Conference*, vol. 3, pp. 277-287.

Zhang, J.S., G.J. Wu, and L.L. Christianson. 1992. Full-scale experimental results on the mean and turbulent characteristics of ventilation flows. *ASHRAE Transactions* 98(2): 307-318.

Zhang, R.H., L.L. Christianson, J.S. Zhang, B. Shaw, and D.L. Day. 1993. Applications of mass transfer principles on modelling gaseous from indoor materials. *Indoor Air '93, Proceedings of the 6th International Conference on Indoor Air and Climate*, vol. 2, Helsinki, Finland.